IEEE Photonics Journal
An IEEE Photonics Society Publication

Open Access

Perfect Anomalous Absorption of TM Polarized Light in Metallic Grating Situated in Asymmetric Surroundings

Volume 6, Number 6, December 2014

Jing Nie
Hu-Quan Li
Wen Liu

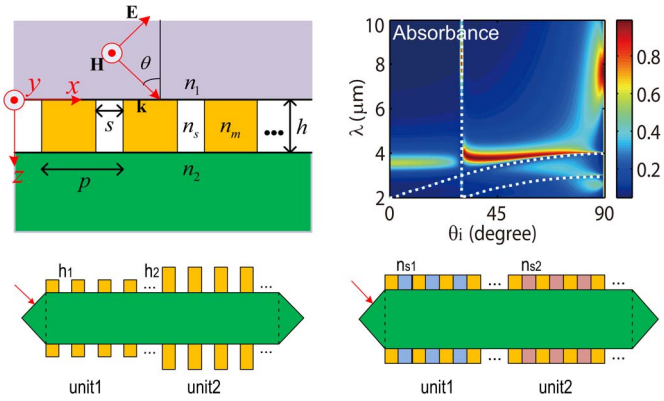

DOI: 10.1109/JPHOT.2014.2363439
1943-0655 © 2014 IEEE

Perfect Anomalous Absorption of TM Polarized Light in Metallic Grating Situated in Asymmetric Surroundings

Jing Nie,[1] Hu-Quan Li,[1] and Wen Liu[1,2]

[1]Wuhan National Laboratory for Optoelectronics, School of Optical and Electronic Information, Huazhong University of Science and Technology, Wuhan 430074, China
[2]School of Physical Sciences, University of Science and Technology of China, Hefei 230026, China

DOI: 10.1109/JPHOT.2014.2363439
1943-0655 © 2014 IEEE. Translations and content mining are permitted for academic research only. Personal use is also permitted, but republication/redistribution requires IEEE permission. See http://www.ieee.org/publications_standards/publications/rights/index.html for more information.

Manuscript received August 19, 2014; revised October 4, 2014; accepted October 9, 2014. Date of publication October 16, 2014; date of current version October 28, 2014. This work was supported in part by the National Natural Science Foundation of China under Grant 11044009/A040507, by the Chinese National Science and Technology Plan 863 under Grant 2011AA010304, and by the China Scholarship Council. Corresponding author: W. Liu (e-mail: liuwen.316@163.com).

Abstract: In this paper, we predict an unexpected perfect optical absorption phenomenon of oblique-incident transverse magnetic polarized light in a metallic grating situated in asymmetric surroundings. Two physical processes result in the anomalous absorption: One is the total internal reflection at the grating's interface; another is the Fabry–Pérot-like resonance supported in the grating's slits. For small filling factor grating $(f < 0.9)$, the enhanced anomalous absorption only appears at grazing incidence with incident angle larger than 85°; however, if the filling factor is sufficiently large $(f > 0.9)$, anomalous absorption is realizable only if the total internal reflection occurs. The influences of structural parameters, such as grating thickness, slits material on the anomalous absorption are investigated. Based on these properties, a plasmonic absorption device with a designed absorption line shape is proposed.

Index Terms: Anomalous absorption, total internal reflection, plasmonic critical angle, FP-like resonance.

1. Introduction

Extraordinary optical transmission (EOT) [1]–[3] and extraordinary optical absorption (EOA) [4]–[9] phenomena for light transmitting through metallic films with subwavelength apertures have been extensively investigated in recent years. The physical mechanisms are widely considered to be the excitation of surface plasmons (SPs) [1]–[3] or spoof SPs (SSPs) for highly conducting metals [10], and or the Fabry–Pérot (FP)-like cavity modes (CMs) resonances in the defects [4], [6], [11]–[13]. Additional mechanism to tunnel light by the high magnetic field concentrated around the metallic films is also evidenced [14], [15]. One common feature of these investigations is that the whole structures are free-standing in air, i.e., both the refractive indexes of incident and output regions equal to unity, we name it as symmetric surroundings (SS).

One of the charming phenomenon for a one-dimensional metallic gratings in SS is the ultra-broadband transmission of light at plasmonic Brewster angle [16]–[19]. However, the plasmonic Brewster angle is usually very large and the oblique-incidence geometry may be not desirable in many situations. One solution to this problem is by situating the metallic grating in asymmetric

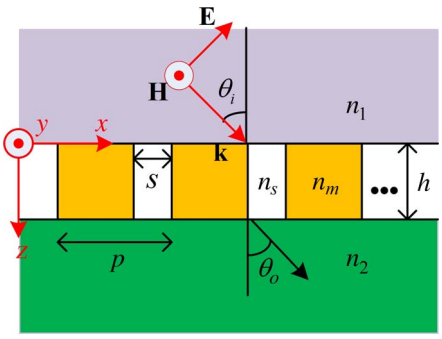

Fig. 1. Schematic diagram of the metallic grating situated in ASS with period p, slit width s, and grating thickness h. Refractive indexes of the input surrounding, output surrounding, metal, and slits are n_1, n_2, n_m, and n_s, respectively. n_2 and n_s are fixed at unity throughout the paper. θ_i is the incident angle, where θ_o is the diffraction angle of fundamental mode.

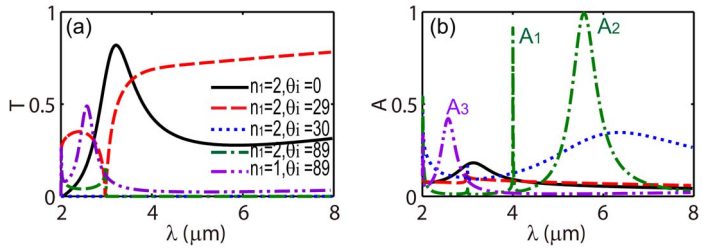

Fig. 2. Transmittance (a) and absorbance (b) of a TM polarized light incident on a metallic grating with structural parameters of $p = 1$ μm, $s = 0.2$ μm, and $h = 1$ μm and surroundings of $n_1 = 2$ and $n_s = n_2 = 1$ at different incident angles. The purple dash-dot-dotted line corresponds to a SS case $(n_1 = n_2 = 1)$.

surroundings (ASS) with different materials for input and output regions [20]. In such a geometry, the plasmonic Brewster angle for a broadband transmission can be surprisingly modulated close to the plasmonic critical angle (PCA) where total internal reflection occurs. However, the optical responses (transmission, reflection, and absorption) of such a subwavelength metallic grating situated in a ASS are far from full understanding.

In this paper, we devote to investigate the optical response of a metallic grating in ASS to the TM polarized light. The general geometry under investigation is shown in Fig. 1. It consists of a gold grating of refractive index n_m, sandwiched between a dense and rarefied surroundings with refractive indexes n_1 and $n_2 = 1$ $(n_1 > n_2)$ on the top and bottom, respectively. TM-polarized light incidents on the structure with oblique angle θ_i. This is a practical scenario in which the total internal reflection and plasmonic critical angle concepts are applied. In practice, a superstrate prism may be necessary to efficiently couple light into the structure. Ultrabroadband transmission phenomenon with plasmonic Brewster angle been greatly reduced close to the plasmonic critical angle is observed. However, this is not the emphasis of this paper. Unexpectedly, if the filling factor of the grating is relative small $(f = (p - s)/p = 0.8)$, an anomalous perfect absorption peak is observed when the incident light grazes on the grating's surface. For a larger filling factor grating $(\mathrm{f} = 0.95)$, however, the anomalous perfect absorption can be realized in a wide oblique angular range. In this paper, we are motivated to investigate the physical mechanism of this perfect anomaly absorption and its dependence on the geometric parameters.

2. Anomalous Absorption Phenomenon

The propagation of electromagnetic field though the structure is calculated by rigorous coupled wave analysis (RCWA) method [21]. The complex refractive index of gold is taken from Palik [22]. In Fig. 2, the transmission and absorption characteristics at different oblique incident

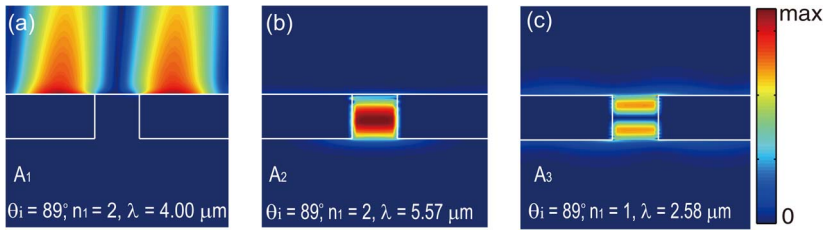

Fig. 3. Non-propagating field distributions |Im(**P**)| at the three resonant absorption peaks A_1, A_2, and A_3.

angles are plotted. The structural parameters are given as $p = 1$ μm, $s = 0.2$ μm, $h = 1$ μm, $n_1 = 2$, and $n_s = n_2 = 1$. For a normal incident light (black solid line), one resonant transmission peak appears in Fig. 2(a), which is physically identified as the first-order FP-like resonant mode supported in the grating's slits. At the same wavelength, a small absorption peak is observed in Fig. 2(b).

When the incident angle is gradually increased close to the PCA (obtained as $\theta_c = \arcsin(n_2/n_1) = 30^\circ$ according to the total internal reflection theory), as can be seen, ultrabroadband transmission is realized in Fig. 2(a) (red dashed line). This phenomenon has been clearly clarified as the broadband impedance match in the structure by Andrea Alù [16], [17]. After that, no light transmits through the gold grating when the incident angle is larger than θ_c only if the subwavelength condition $\lambda > \lambda_{\mathrm{T-RA_1}} = p(n_1 \sin\theta_i + n_2)$ is satisfied. Since total internal reflection occurs on the bottom interface of the grating. $\lambda_{\mathrm{T-RA_1}}$ represents the wavelength of the first-order transmission Rayleigh anomaly $(\mathrm{T\text{-}RA_1})$ [20]. However, according to the absorption lines presented in Fig. 2(b) (the blue dotted line), not all of the energy is reflected to the input surrounding, which indicates some of the energy is confined in the grating.

More surprisingly, when the incident angle is increased to a grazing incidence $(\theta_i > 80^\circ)$, unexpected optical response, i.e., inherently resonant absorptions are observed (green dash-dotted line). One of the absorption peaks at $\lambda \approx 4$ μm (A_1) corresponds to the first-order reflection Rayleigh anomaly $(\mathrm{R\text{-}RA_1})$ [20] that can be quantitatively predicted as $\lambda = pn_1(1 + \sin\theta_i)$. It indicates the reflection off of the first-order diffraction. As for the second absorption peak locates at $\lambda = 5.57$ μm (A_2), the physical origin is not clear and need to be explored. As a comparison, the results of a gold grating in a SS $(n_1 = n_2 = 1)$ at the grazing incidence $(\theta_i = 89^\circ)$ are presented (purple dash-dot-dotted line), which contains a FP-like resonant transmission peak and a FP-like resonant absorption peak A_3.

3. Qualitative Speculation and Quantitative Interpretation

3.1. Qualitative Speculation

In order to give insight into the characteristics and physical origins of the two absorption peaks for grazing incidence, we calculate the absolute of imaginary part of the Pointing vector $|\mathrm{Im}|(\mathbf{P})| = \sqrt{[\mathrm{Im}(P_x)]^2 + [\mathrm{Im}(P_z)]^2}$ as shown in Fig. 3, which contains information about the non-propagating fields and local resonances near the plasmonic structure [23]. For absorption peak A_1, the non-propagating field is clearly localized near the top interface of the metallic grating, indicating the properties of the reflection Rayleigh anomaly. For the second absorption peak A_2, however, the non-propagating field is highly confined in the grating's slits, which indicates the physical origin to be a local resonance supported in the slits. As a comparison, the non-propagating field distribution corresponding to the FP-like resonant absorption peak A_3 is presented in Fig. 3(c), where total internal reflection does not occur. Considering the practical difference between the scenarios of absorption peaks A_2 and A_3, and comparing the non-propagating field distributions between them, we make a speculation that resonant mode A_2 has the same physical origin of FP-like resonance as that of A_3.

3.2. Quantitative Interpretation

To verify this speculation, we develop a quantitative model based on transmission line approach [16], [24] to model the scattering performance of such a periodic structure in ASS and analyze the anomaly absorption. Following Alù [16], for a TM polarized light incident at angle θ_i, the transverse characteristic impedances of the input and output surroundings normalized to the grating period are defined as

$$\eta_{in} = \frac{\eta_0}{n_1} p \cos\theta_i, \eta_{out} = \frac{\eta_0}{n_2} p \sqrt{1 - \frac{n_1^2 \sin^2\theta_i}{n_2^2}}. \tag{1}$$

In subwavelength regime, the field inside the slits is expanded with the propagation mode supported in the metal–insulator–metal waveguide. The wavevector of the guide mode β_s can be calculated from the transcendental equation

$$\tan\left(\sqrt{k_0^2 n_s^2 - \beta_s^2}\frac{s}{2}\right) = \frac{n_s^2}{n_m^2}\frac{\sqrt{\beta_s^2 - k_0^2 n_m^2}}{\sqrt{k_0^2 n_s^2 - \beta_s^2}} \tag{2}$$

then the grating layer can be treated as a homogenous slab with transverse characteristic impedance

$$\eta_s = \frac{V_s}{I_s} = \frac{\beta_s s}{\omega\varepsilon_0 n_s^2} \tag{3}$$

which is defined as the ratio between the effective voltage $V_s = \int_0^s E_x dx$ and the effective current $I_s = \omega\varepsilon_0 n_s^2 E_x/\beta_s$. E_x is the x-component of electric field.

In this equivalent picture of a homogenous slab in ASS, the elementary Fresnel reflection and transmission coefficients of TM polarized light at the top interface can be expressed as [24]

$$\rho_{T1} = \frac{\eta_s - \eta_{in}}{\eta_s + \eta_{in}}, \tau_{T1} = \frac{2\eta_{in}}{\eta_s + \eta_{in}}. \tag{4}$$

Similarly, at the bottom interface

$$\rho_{T2} = \frac{\eta_{out} - \eta_s}{\eta_{out} + \eta_s}, \tau_{T2} = \frac{2\eta_s}{\eta_{out} + \eta_s} \tag{5}$$

accordingly, the total reflection and transmission coefficients of the equivalent uniform slab for TM polarized light can be obtained by rigorously calculating the Maxwell equation and matching the boundary conditions on the interfaces (the continuity of transverse components of electric and magnetic fields), which is given as

$$r_T = -\frac{\rho_{T1} + \rho_{T2} e^{-j2\delta_1}}{1 + \rho_{T1}\rho_{T2} e^{-j2\delta_1}}, t_T = \frac{\tau_{T1}\tau_{T2} e^{-j\delta_1}}{1 + \rho_{T1}\rho_{T2} e^{-j2\delta_1}}. \tag{6}$$

Being cautious, one may notice that the total reflection coefficient is different from those given by Orfanidis [24] and Argyropoulos [16]. The pre-minus in r_T is rigorous for TM polarized light, even though it does not affect the final reflectance of a single slab since it is the square of the modulus of r_T. $\delta_1 = \beta_s h$ is the propagation phase in the equivalent slab. Substituting (4) and (5) into (6), the results are reduced to

$$\begin{aligned} r_T &= -\frac{i\left(\eta_s^2 - \eta_{in}\eta_{out}\right)\tan\delta_1 - \eta_s(\eta_{in} - \eta_{out})}{i\left(\eta_s^2 + \eta_{in}\eta_{out}\right)\tan\delta_1 + \eta_s(\eta_{in} + \eta_{out})} \\ t_T &= \frac{2\eta_{in}\eta_s \sec\delta_1}{i\left(\eta_s^2 + \eta_{in}\eta_{out}\right)\tan\delta_1 + \eta_s(\eta_{in} + \eta_{out})} \end{aligned} \tag{7}$$

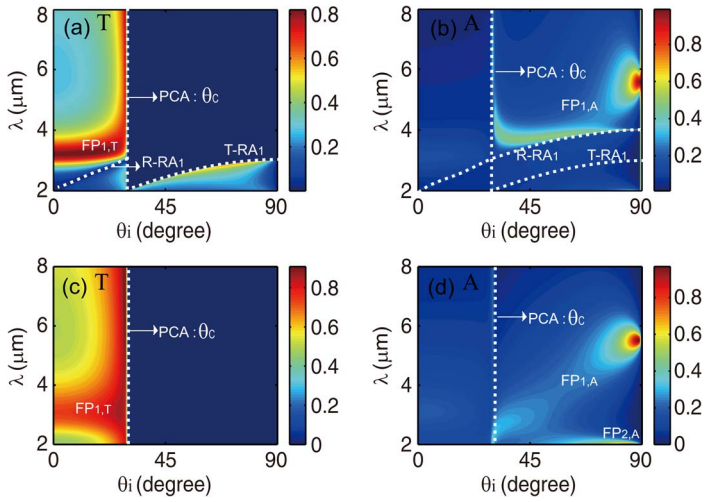

Fig. 4. Scanning maps of transmittance (T) and absorbance (A) based on RCWA method [(a) and (b)] and transmission line model [(c) and (d)] with parameters of wavelength and incident angle. Other parameters are given as $p = 1$ μm, $s = 0.2$ μm, $h = 1$ μm, $n_1 = 2$, and $n_s = n_2 = 1$. FP_1 and FP_2 indicate the first- and second-order FP resonances, respectively.

then the total reflectance R and transmittance T are computed as

$$R = |r_T|^2, T = \mathrm{Re}\left(\frac{\cos\theta_o}{\cos\theta_i}\frac{n_1}{n_2}\right)|t_T|^2. \tag{8}$$

According to energy conservation, absorbance is calculated as $A = 1 - R - T$.

In Fig. 4, the scanning maps of transmittance and reflectance with parameters of wavelength and incident angle are presented. Fig. 4 (a) and (b) are calculated from RCWA method. The theoretical predictions based on the transmission line model (see (7) and (8)) are presented in Fig. 4(c) and (d). Apparently, in the subwavelength regime, transmission line mode gives good prediction of the FP-like resonant transmission $(FP_{1,T})$ and ultrabroadband funneling light through the metallic grating for incident angle near the PCA [see Fig. 4(a) and (c)]. When the incident angle is larger than PCA, total internal reflection occurs and light cannot transmit through the structure theoretically, except in the nonsubwavelength region $(\lambda < \lambda_{T-RA_1})$ where higher orders of diffraction waves become propagative [see Fig. 4(a)]. In this angular range $(\theta > \theta_C)$, the incident light in subwavelength regime is either reflected to the input surrounding, or confined and exhausted in the grating layer.

From Fig. 4(b), it is clearly shown that light is partially absorbed at the first-order FP-like cavity resonance for incident angle between 30° and 80°, which is labeled as $FP_{1,A}$. If the incident angle becomes larger than 80°, a stronger absorption peak bumps up in the longer wavelength region unexpectedly (A_2). The scanning map obtained from transmission line model predicts this absorption peak very well [see Fig. 4(d)].

According to the characteristics presented in Fig. 4(b) and (d), the absorption peak A_2 is obviously resonant in nature. Considering the equivalent approach we have made in the transmission line model, i.e., the grating layer has been equaled to a homogenous slab with transverse characteristic impedance η_s, FP resonance is the only one possible category of resonance supported in the equivalent structure. Consequently, the absorption peak near $\lambda = 5.6$ μm in Fig. 4(d) is physically the first-order FP resonant absorption in nature, such as that of the absorption peak near $\lambda = 5.6$ μm in Fig. 4(b).

Consequently, absorption peak A_2 is physically the first-order FP-like resonance supported in the grating slits. The obvious redshift of FP_1 at grazing incidence is qualitatively ascribed to the additional phase gained at the openings of the slits during a round trip [25]. The anomalous

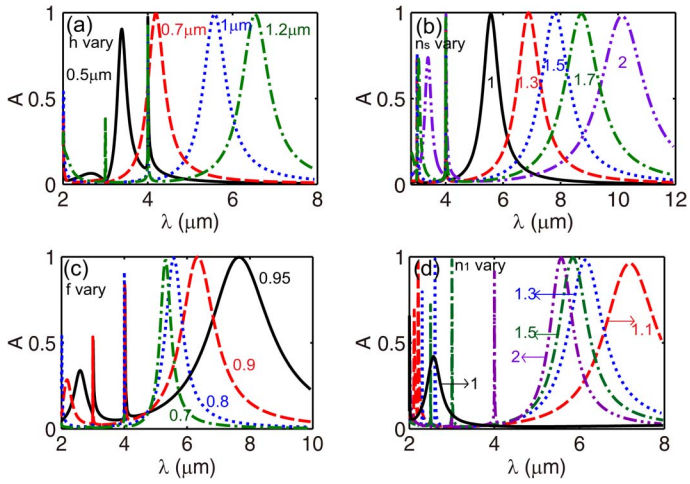

Fig. 5. Influences of structural parameters such as grating thickness h (a), slits refractive index n_s (b), grating's filling factor $f = (p - s)/p$ (c), and the influence of the input surrounding n_1 (d) on the anomalous absorption peak A_2. Other parameters are given as (a) $p = 1$ μm, $s = 0.2$ μm, $n_1 = 2$, $n_s = n_2 = 1$; (b) $p = 1$ μm, $s = 0.2$ μm, $h = 1$ μm. (c) $p = 1$ μm, $h = 1$ μm, $n_1 = 2$, $n_s = n_2 = 1$; (d) $p = 1$ μm, $s = 0.2$ μm, $h = 1$ μm, $n_s = n_2 = 1$.

absorption peak corresponds to the reflection minimum that can be quantitatively predicted by (7). However, our model cannot predict the absorption peak A_1, since the reflection Rayleigh anomaly originating from the first order of diffraction wave.

4. Influence of Structural and Surrounding's Parameters on the Anomalous Absorption

Since we have explained the physical origin of the anomalous absorption peak A_2 at grazing incidence $(\theta = 89^\circ)$, in Fig. 5, we investigate the influences of structural and surrounding's parameters on it. Fig. 5(a) presents the influence of grating's thickness h. Apparently absorption peak A_2 is red-shifted as the grating's thickness increases, indicating the FP resonant nature. However, the absorption peak A_1 is fixed during the thickness increasing. Another way to modulate the position of absorption peak A_2 is by changing the filling material in the slits. It can increase the effective cavity length as the refractive index n_s increases, and consequently, the absorption peak A_2 is red-shifted [see Fig. 5(b)]. Meanwhile, the second-order of FP-like resonant absorptions are also observed in Fig. 5(b) when the cavity length is sufficiently large (the green dash-dotted line and the purple dash-dot-dotted line).

In Fig. 5(c), the influence of the grating's filling factor $f = (p - s)/p$ is explored. As presented, smaller filling factor (larger slit width) blueshifts the absorption peak, since the effective index of the guide mode in the slits decreases when the slits width increases. Meanwhile, the full-width at half-maximum (FWHM) bandwidth is narrowed for smaller filling factor, since the evanescent wave on the slits walls gets decoupled and fewer lights around the guide mode's central wavelength can propagate through the slits.

Fig. 5(d) shows the influence of the input surrounding which directly affects the PCA of the structure. For the SS case, since the input and output surroundings are the same, total internal reflection does not occur. As a consequence, the grazing incident light only experiences a small absorption around $\lambda = 2.58$ μm (black solid line). Nearly the same portion of energy is resonantly transmitted (not shown here). However, if the index of input surrounding is larger than that of output surrounding, total internal reflection occurs and the FP-like resonant absorption is greatly redshifted to longer wavelength regime (red dashed line). This is because the slits are not rigorous FP cavities and the resonant position is highly dependent on the additional phase accumulated at the ends of the slits [25], especially when total reflection occurs at the ends. If

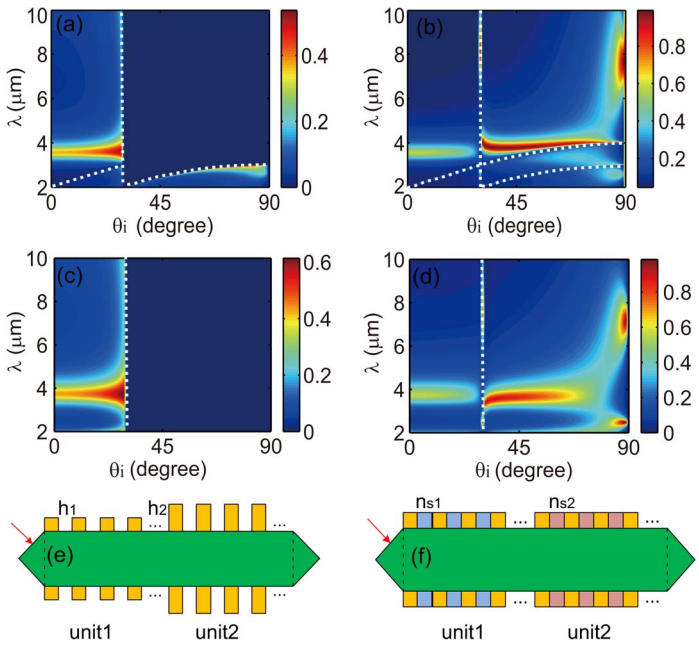

Fig. 6. Transmittance (a) and absorbance (b) scanning maps for a TM-polarized light incident on a metallic grating with parameters of wavelength and incident angle. Other parameters are given as $p = 1$ μm, $s = 0.05$ μm, $h = 1$ μm. Surrounding materials are $n_1 = 2$ and $n_s = n_2 = 1$. (c) and (d) Corresponding results calculated from transmission line model. (e) and (f) Schematic diagrams proposed for arbitrary multiband absorption plasmonic devices.

we further increase the index of input surrounding, the resonant wavelength is gradually blueshifted due to the changing of additional phase.

The results presented above show that a metallic grating situated in a ASS supports greatly enhanced perfect absorption for TM polarized light at grazing incidence. For smaller incident angles, however, the absorption is not effectively enhanced [see Fig. 4(b)]. The grazing incidence condition may increase the difficulty in practical applications. However, it does not mean that the FP-like resonant absorption can be enhanced only at grazing incidence. In Fig. 6, the scanning maps of transmittance and absorbance of the same structure but different filling factors are presented. Here the filling factor is increased to $f = 0.95$. Other parameters are $p = 1$ μm, $h = 1$ μm, $n_1 = 2$ and $n_s = n_2 = 1$. We can see that for a larger filling factor (narrower slits), when the incident angle is larger than PCA (i.e., total internal reflection occurs), the initial resonant transmitted energy is well confined to the grating and strong FP-like resonant absorption is realized [see Fig. 6(b)]. The corresponding transmission and absorption spectrums calculated from transmission line model are presented in (c) and (d), respectively. We can see they agree well with the results calculated from RCWA method.

According to the properties of the FP-like resonant absorption peak A_2, multiband absorption plasmonic devices may be designed, as shown in Fig. 6(e) and (f). By tuning the grating's thickness or materials filled in the slits in each unit to change the effective cavity length, arbitrary absorption line shape is theoretically realizable for practical applications. The prism-like ends of the dielectric slab is designed to efficiently couple light in or out of the structure. A red arrow represents the incidence of light.

5. Conclusion

In conclusion, we have predicted unexpected absorption phenomenon for oblique incident TM polarized light impinging on a one-dimensional metallic grating situated in ASS. The anomalous absorption is physically ascribed to the redshifted FP-like resonant mode supported in the

grating's slits. When the oblique incident angle is larger than PCA, the total internal reflection occurs and no light can transmit through the structure. As thus, the anomalous absorption exactly corresponds to the reflection minimum. A transmission line model is developed to interpret the perfect anomalous absorption quantitatively. The geometry parameters, such as grating thickness, filling factor, slits material could be tuned to modulate the absorption for different applications. Basing on these properties, an absorptive plasmonic device with arbitrary absorption line shape is theoretically proposed.

References

[1] T. W. Ebbesen, H. J. Lezec, H. F. Ghaemi, T. Thio, and P. A. Wolff, "Extraordinary optical transmission through sub-wavelength hole arrays," *Nature*, vol. 391, no. 6668, pp. 667–669, Feb. 1998.

[2] W. L. Barnes, A. Dereux, and T. Ebbesen, "Surface plasmon subwavelength optics," *Nature*, vol. 424, pp. 824–830, Aug. 2003.

[3] J. A. Porto, F. J. Garcia-Vidal, and J. B. Pendry, "Transmission resonances on metallic gratings with very narrow slits," *Phys. Rev. Lett.*, pp. 2845–2848, Oct. 1999.

[4] H.-Q. Li and J.-S. Liu, "Unexpected strong optical absorption in a free-standing optical thick transmission metallic grating," *IEEE Photon. J.*, vol. 6, no. 2, pp. 1–8, Apr. 2014.

[5] H.-Q. Li, K.-J. Wang, Z.-G. Yang, and J.-S. Liu, "Unexpected unidirectional perfect absorption of light in a freestanding optical thin metallic grating with extremely small filling factor," *J. Opt. Soc. Amer. B*, vol. 31, no. 4, pp. 806–809, Mar. 2014.

[6] J. Nie, H.-Q. Li, and W. Liu, "Robust broadband optical transmission realized in a dual-metallic gratings structure," *IEEE Photon. J.*, vol. 6, no. 4, pp. 1–8, Aug. 2014.

[7] C. Argyropoulos, K. Q. Le, N. Mattiucci, G. D'Aguanno, and A. Alù, "Broadband absorbers and selective emitters based on plasmonic Brewster metasurfaces," *Phys. Rev. B*, vol. 87, no. 20, p. 205112, May 2013.

[8] K. Aydin, V. E. Ferry, R. M. Briggs, and H. a Atwater, "Broadband polarization-independent resonant light absorption using ultrathin plasmonic super absorbers," *Nat. Commun.*, vol. 2, p. 517, Jan. 2011.

[9] Y. Cui *et al.*, "Ultrabroadband light absorption by a sawtooth anisotropic metamaterial slab," *Nano Lett.*, vol. 12, no. 3, pp. 1443–1447, Mar. 2012.

[10] J. B. Pendry, L. Martín-Moreno, and F. J. Garcia-Vidal, "Mimicking surface plasmons with structured surfaces," *Science (80-.)*, vol. 305, no. 5685, pp. 847–848, Aug. 2004.

[11] J. Bravo-Abad, L. Martín-Moreno, and F. García-Vidal, "Transmission properties of a single metallic slit: From the subwavelength regime to the geometrical-optics limit," *Phys. Rev. E.*, vol. 69, no. 2, p. 026601, Feb. 2004.

[12] B. Hou *et al.*, "Tuning Fabry–Perot resonances via diffraction evanescent waves," *Phys. Rev. B*, vol. 76, no. 5, p. 054303, Aug. 2007.

[13] X.-R. Huang, R.-W. Peng, and R.-H. Fan, "Making metals transparent for white light by spoof surface plasmons," *Phys. Rev. Lett.*, vol. 105, no. 24, p. 243901, Dec. 2010.

[14] L. Zhou, W. Wen, C. Chan, and P. Sheng, "Electromagnetic-wave tunneling through negative-permittivity media with high magnetic fields," *Phys. Rev. Lett.*, vol. 94, no. 24, p. 243905, Jun. 2005.

[15] D. L. Gao, L. Gao, and C. W. Qiu, "Birefringence-induced polarization-independent and nearly all-angle transparency through a metallic film," *EPL*, vol. 95, no. 3, p. 34004, Aug. 2011.

[16] C. Argyropoulos *et al.*, "Matching and funneling light at the plasmonic Brewster angle," *Phys. Rev. B*, vol. 85, no. 2, p. 024304, Jan. 2012.

[17] A. Alù, G. D'Aguanno, N. Mattiucci, and M. J. Bloemer, "Plasmonic Brewster angle: Broadband extraordinary transmission through optical gratings," *Phys. Rev. Lett.*, vol. 106, no. 12, p. 123902, Mar. 2011.

[18] X.-R. Huang, R.-W. Peng, and R.-H. Fan, "Making metals transparent for white light by spoof surface plasmons," *Phys. Rev. Lett.*, vol. 105, no. 24, p. 243901, Dec. 2010.

[19] K. Q. Le *et al.*, "Broadband Brewster transmission through 2D metallic gratings," *J. Appl. Phys.*, vol. 112, no. 9, p. 094317, 2012.

[20] Z. Wang *et al.*, "Plasmonic critical angle in optical transmission through subwavelength metallic gratings," *Opt. Lett.*, vol. 36, no. 23, pp. 4584–4586, 2011.

[21] M. G. Moharam, E. B. Grann, D. A. Pommet, and T. K. Gaylord, "Formulation for stable and efficient implementation of the rigorous coupled-wave analysis of binary gratings," *J. Opt. Soc. Amer. A*, vol. 12, no. 5, p. 1068–1076, May 1995.

[22] E. Palik, *Handbook of Optical Constants of Solids*. San Diego, CA, USA: Academic, 1998.

[23] [Online]. Available: http://docs.lumerical.com/en/layout_analysis_poynting_vector.html?zoom_highlightsub=poynting

[24] S. Orfanidis, *Electromagnetic Waves and Antennas*. New Brunswick, NJ, USA: Rutgers Univ. Press, 2002.

[25] J. Nie and W. Liu, "Origin of the positional offset of FP-like enhanced transmission peaks in a one-dimensional gold grating," *J. Mod. Opt.*, vol. 60, no. 21, pp. 1850–1854, Dec. 2013.